Chapter 9

Magnetic-Based Contact and Non-Contact Manipulation of Cell Mockups and MCF-7 Human Breast Cancer Cells

Islam S. M. Khalil, Iman E. O. Gomaa,
Reham M. Abdel-Kader and Sarthak Misra

Additional information is available at the end of the chapter

http://dx.doi.org/10.5772/61686

Abstract

The use of wireless magnetic control to transport and deliver chemotherapeutic agents selectively to tumor cells has become a promising strategy to mitigate the negative side effects associated with conventional treatment. It is necessary to manipulate and penetrate biological cells using magnetic agent to achieve this targeted drug delivery. Contact and non-contact micromanipulation of cell mockups and biological cells (human astrocytoma cell line U-373 MG and human breast adenocarcinoma cell line MCF-7) is achieved using magnetic agents (paramagnetic microparticles and iron oxide nanoparticles). The contact manipulation is accomplished under the influence of the controlled magnetic field gradients exerted on the magnetic agent, whereas the non-contact manipulation is done under the influence of the magnetic field and pressure gradients exerted on the agent and biological cells, respectively. We develop a magnetic-based teleoperation system that allows us to control the motion of the magnetic agents using microscopic feedback. This teleoperation is used to manipulate cell mockups toward reference positions in the presence and absence of contact between the cells and the magnetic agents. In addition, we demonstrate that iron oxide nanoparticles selectively move toward an MCF-7 cell and penetrate its walls without permanently damaging the membrane. This penetration is achieved in 28 seconds using controlled external magnetic fields and under microscopic vision guidance. The precise non-contact manipulation of biological cells using microparticles provides broad possibilities in targeted therapy and biomedical applications that require successful releases and selective penetration of cells without causing a permanent damage to the membrane.

Keywords: Magnetic, Breast cancer cells, motion control, wireless, magnetic forces, manipulation, non-contact, drug delivery

1. Introduction

Manipulation at microscale can be used in diverse biomedical, e.g., manipulation and positioning of biological cells in an aqueous environment and targeted drug delivery (Fig. 1), and nanotechnology applications [1, 2, 8]. One of the main challenges that prevent the automation of manipulation at microscale is the difficulty to make successful releases at the desired position due to the adhesive forces [9]. These adhesive forces result in stickiness between the tips of the manipulator and the manipulated object and thus prevent the release of the object in the desired position. Several techniques have been introduced to overcome the effect of the dominant adhesive forces. Saito et al. have proposed the utilization of voltage between the end effector and the substrate to produce an electric field that assists the sample release [10]. Kim et al. have reduced the adhesion between biological cells and microgripper tips by dip coating the tips with 10% SurfaSil siliconizing fluid and 90% histological-grade xylenes for 10 seconds before use [11]. Magnetic microrobotic systems have been also used in micromanipulation to push and pull the microobject toward the desired positions [2, 12]. Khalil et al. have demonstrated contact micromanipulation of nonmagnetic (SU-8) microobjects using clusters of paramagnetic microparticles using an orthogonal array of electromagnetic coils [5]. It has also been shown that these microparticles can be used to achieve a microassembly of microobjects. However, it is difficult to achieve successful releases and decrease the completion time of the microassembly tasks.

Manipulation using magnetic agents can be classified into two categories, i.e., contact [13] and non-contact manipulation [14, 29]. In contact manipulation, the presence of adhesive forces prevents the release of the microobjects, whereas in non-contact manipulation, it is relatively easy to break free from the adhesive force and achieve successful releases.

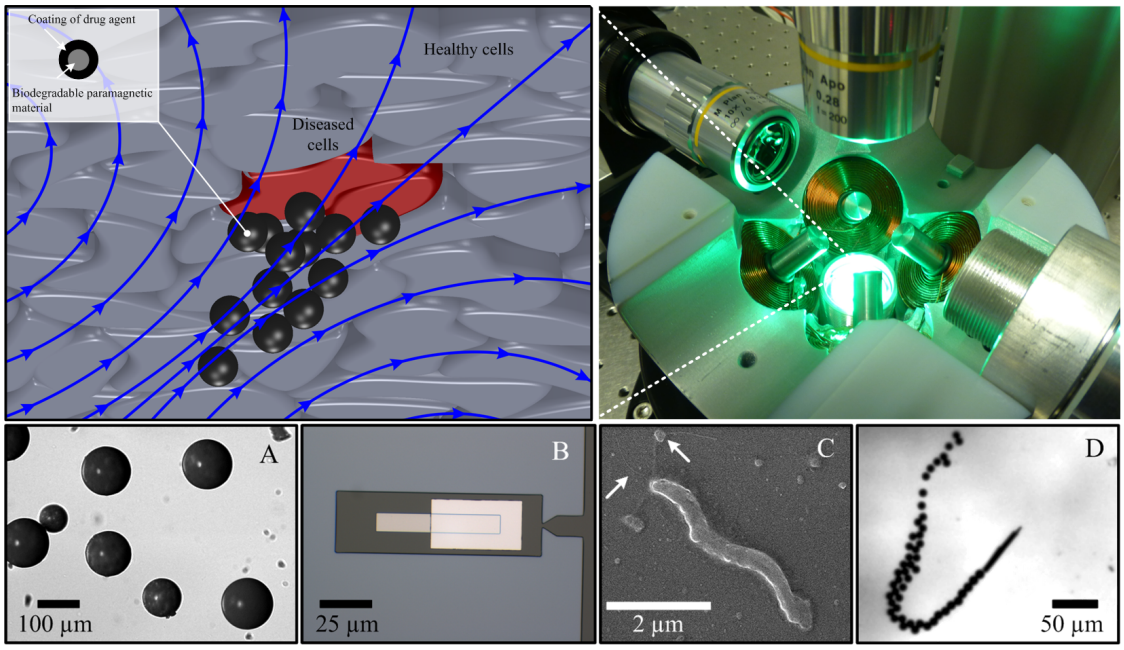

Figure 1. A schematic representation of targeted drug delivery using magnetic microparticles. The microparticles move toward the diseased cells (red) without affecting the healthy cells (gray). This level of control is achieved under the influence of the controlled magnetic forces (emanating from the electromagnetic system [15]) exerted on the magnetic dipole of the microparticles. The following magnetic agents can also be used to achieve targeted drug delivery: (a) microparticles, (b) magnetic microrobots, (c) magnetotactic bacteria [16], and (d) self-propelled microrobots [31].

http://dx.doi.org/10.5772/61686

Gazzar et al. have demonstrated that non-contact micromanipulation of nonmagnetic beads can be achieved using a transition between low and high Reynolds numbers [29]. First, the magnetic agents achieve non-contact pushing or pulling at low Reynolds number (by moving slowly). Second, the control system increases the speed of the magnetic agent once the nonmagnetic bead is positioned at the reference position to break free from the adhesive forces. Two-dimensional contact and non-contact micromanipulation of microspheres using a mobile microrobot has been achieved by Floyd et al. [14]. In the contact mode, the microrobot has been used to push the microspheres, whereas in the non-contact mode, the fluid flow caused by the translation of the microrobot generates enough force to push the microspheres. However, this non-contact manipulation has not been implemented using multiple microrobotic agents (microparticles) to control the non-contact driving forces (by changing the number of microparticles within the cluster) on the microobjects and to allow for coarse and fine non-contact positioning.

In this study, we achieve the following:

1. Development of a magnetic-based teleoperation system for the contact and non-contact manipulation of cell mockups and MCF-7 human breast cancer cells
2. Characterization of the motion control specifications of the contact and non-contact manipulation in the transient and steady states
3. Analyzing the relation between the speed of non-contact manipulation for different numbers of microparticles within the cluster during pushing and pulling

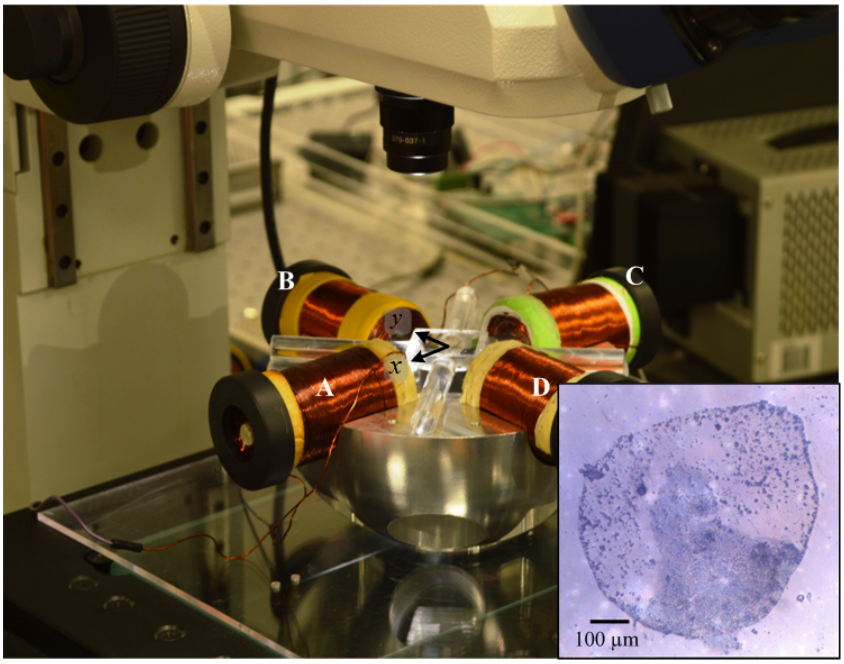

Figure 2. An electromagnetic system for the contact and non-contact manipulation and penetration of U-373 MG cells and MCF-7 cells. The system consists of an orthogonal array of electromagnetic coils with iron cores. The electromagnetic configuration surrounds a reservoir that contains the cells (or the cell mockups) and the magnetic agents. Position of the cells and magnetic agents is determined using a microscopic unit (MF Series 176 Measuring Microscopes, Mitutoyo, Kawasaki, Japan) and a high-speed camera (avA1000-120kc, Basler Area Scan Camera, Basler AG, Ahrensburg, Germany). The letters A, B, C, and D indicate the electromagnetic coils. The inset shows a human astrocytoma cell line U-373 MG.

4. Selective penetration of MCF-7 cells using clusters of iron oxide nanoparticles.

We present a magnetic-based manipulation technique that allows for the contact and non-contact positioning of biological cells and penetration of the cells without causing damage to its walls. This manipulation is done using an electromagnetic configuration, cell mockups, and human astrocytoma cell line U-373 MG (Fig. 2) and human breast adenocarcinoma cell line MCF-7. The non-contact manipulation of the cell mockups is modeled, and experiments are done for Reynolds number regimes of less and greater than 0.1. In addition, the effect of the distance between the cluster of microparticles and the cell mockup and the number of microparticles within the clusters are investigated. We also fabricate iron oxide nanoparticles and use them in the penetration of the MCF-7 cells under the influence of the controlled magnetic field and using microscopic vision guidance.

The remainder of this chapter is organized as follows: Section 2 provides theoretical and experimental analysis pertaining to the non-contact manipulation of cell mockups using paramagnetic microparticles. The difference between contact and non-contact manipulation is explained and verified experimentally for Reynolds number less and greater than 0.1, in Section 2. The fabrication of iron oxide nanoparticles and the preparation of the U-373 MG and MCF-7 cells are included in Section 3. In addition, this section also includes a proof-of-concept experimental trial on the penetration of an MCF-7 cell using a cluster of nanoparticles, under the influence of the controlled magnetic field gradients. Finally, Section 4 concludes and provides directions for future work.

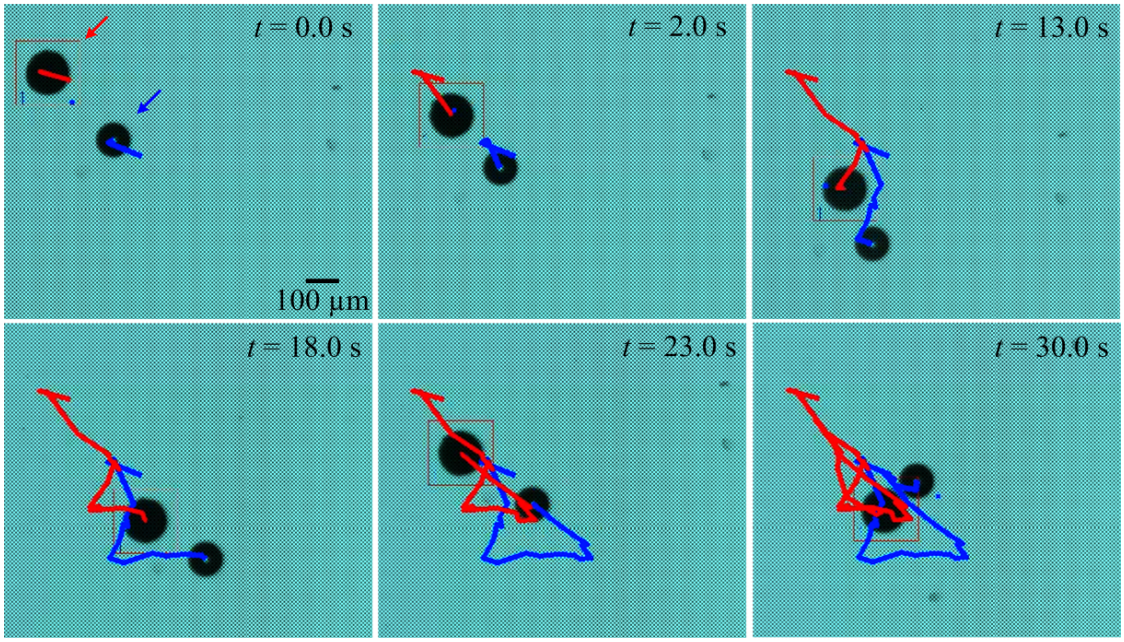

Figure 3. A representative teleoperation experiment of a cell mockup (blue polystyrene particles, Micromod Partikeltechnologie GmbH, Rostock-Warnemunde, Germany) with average diameter of 100 μm using a paramagnetic microparticle (PLAParticles-M-redF-plain, Micromod Partikeltechnologie GmbH, Rostock-Warnemunde, Germany) with average diameter of 100 μm. The teleoperation is achieved without contact between the cell mockup and the microparticle. The red and blue arrows indicate the paramagnetic microparticle and the cell mockup, respectively. At time, t=0.0 seconds, magnetic field gradient is exerted on the paramagnetic microparticle, and non-contact manipulation of the cell mockup is achieved.

http://dx.doi.org/10.5772/61686

2. Modeling and control of the contact and non-contact manipulation

Cell mockups and biological cells can be manipulated, sorted, and fixed for diverse biomedical applications. The motion of the cells is studied under the influence of a moving fluid that is carried by controlled magnetic microparticles at low Reynolds number regime. We also study the effect of the inertia when clusters of microparticles are used to control the position of the cell mockups or biological cells.

2.1. Modeling and characterization of the manipulation

Clusters of magnetic microparticles are subjected to magnetic force $(\mathbf{F}(\mathbf{P}))$ and magnetic torque $(\mathbf{T}(\mathbf{P}))$ under the influence of an external magnetic field $(\mathbf{B}(\mathbf{P}))$, at point $(\mathbf{P})$. The magnetic force exerted on the dipole of the cluster is given by [25]

$$\mathbf{F}(\mathbf{P}) = (\mathbf{m} \cdot \nabla)\mathbf{B}(\mathbf{P}) = (\mathbf{m} \cdot \nabla)\widetilde{\mathbf{B}}(\mathbf{P})\mathbf{I} = \mathbf{\Lambda}(\mathbf{m}, \mathbf{P})\mathbf{I}, \tag{1}$$

where $\mathbf{m} \in \mathbb{R}^{3\times1}$ and $\mathbf{B}(\mathbf{P}) \in \mathbb{R}^{3\times1}$ are the magnetic dipole moment of the cluster of microparticle and the induced magnetic field, respectively [18, 19]. Further, $\mathbf{I}$ is the current input to the electromagnetic coils (Fig. 2) and $\widetilde{\mathbf{B}}(\mathbf{P})$ is the magnetic field-current map. $\mathbf{\Lambda}(\mathbf{m}, \mathbf{P})$ is the magnetic force-current map [2]. The position of the cluster of microparticles is controlled using (1) by pulling using the field gradient, whereas the orientation of the cluster is controlled using the magnetic torque that is given by

$$\mathbf{T}(\mathbf{P}) = \mathbf{m} \times \mathbf{B}(\mathbf{P}) = \mathbf{m} \times \widetilde{\mathbf{B}}(\mathbf{P})\mathbf{I}. \tag{2}$$

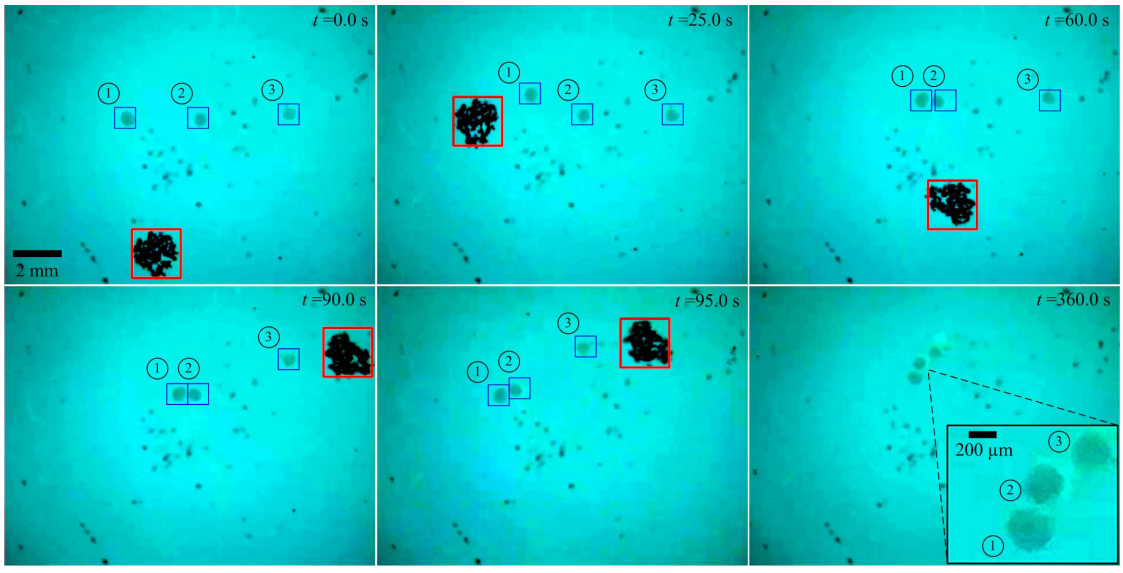

Figure 4. A representative teleoperation experiment of non-contact microassembly of three cell mockups using a cluster of microparticles at different time instants (t). The cluster pushes and pulls the cell mockups without contact under the influence of the controlled magnetic fields to form a row of three cell mockups connected together (at time, t=360 seconds). In this microassembly experiment, the average speed of the cluster is 300 μm/s. The cluster consists of 15 microparticles. Paramagnetic microparticles with average diameter of 100 μm are used in this experiment.

Fig. 3 shows a representative non-contact manipulation using pushing and pulling between a paramagnetic microparticle (PLAParticles-M-redF-plain, Micromod Partikeltechnologie GmbH, Rostock-Warnemunde, Germany) and a nonmagnetic cell mockup (blue polystyrene particles, Micromod Partikeltechnologie GmbH, Rostock-Warnemunde, Germany). At time, t=0.0 seconds, the paramagnetic microparticle is pulled toward the cell mockup. The traces of the paramagnetic microparticle (red) and the cell mockup (blue) indicate that a non-contact force exists. This force allows us to manipulate the cell mockup without contact. At time, t=30 seconds, the adhesive force between the microparticle and the cell mockup dominates, and at this instance, contact manipulation can be used to move the cell mockup. We calculate Reynolds number to understand the non-contact manipulation that is shown in Fig. 3. Reynolds number (R_e) is given by

$$R_e = \frac{2\rho_f v r_p}{\eta}, \tag{3}$$

where v and η are the speed of the microparticle and fluid dynamic viscosity (1 mPa.s), respectively. Further, r_p is the radius of the particle (100 μm) and ρ_f is the density of the fluid. Using (3), Reynolds number is calculated to be less than 0.01 for velocity of 30 μm/s of the paramagnetic microparticle. Therefore, the motion of the microparticle results in

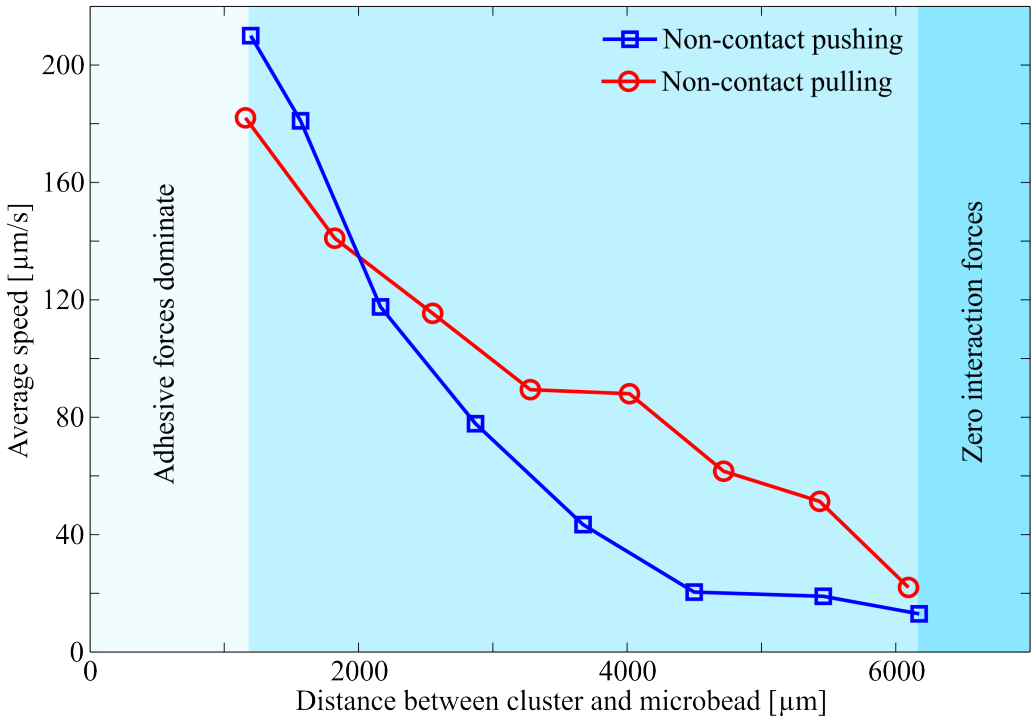

Figure 5. Average speed of the cell mockup versus the distance between the centers of the cluster of microparticles and the cell mockup. A cluster of 10 microparticles is used during pushing and pulling. The speed of the cell mockup is inversely proportional to the distance between the cluster and the cell mockup for the pushing and pulling. The adhesive force dominates for d <1200 μm, and non-contact pushing and pulling cannot be achieved. Non-contact manipulation can be done within 1200 μm< d <6200 μm. Zero interaction force is observed for d >6200 μm. The paramagnetic microparticles have an average diameter of 100 μm [29].

http://dx.doi.org/10.5772/61686

shear and the fluid at the surface of the microparticle moves with the microparticle [20] and hence moves the cell mockup without contact. At time, t=18 seconds, the direction of the microparticle is reversed by the magnetic field gradient. We observe that the cell mockup also reverses its direction and moves with the paramagnetic microparticle. This behavior is attributed to the motion of the fluid within the vicinity of the paramagnetic microparticle, as the fluid is carried with the microparticle. This behavior is only observed at low Reynolds number due to the absence of inertia.

We also investigate the non-contact manipulation of cell mockups for a Reynolds number larger than 0.1. For a cluster of less than 4 microparticles, the Reynolds number is calculated to be 0.024 (at average speed of 120 μm/s). For a cluster of eight microparticles, the Reynolds number is calculated to be 0.19 (at average speed of 494 μm/s). The Reynolds number at these two representative numbers of microparticles indicates that the inertial effect in the fluid could influence the non-contact manipulation of the nonmagnetic cell mockup based on the number of microparticles in the cluster. Fig. 4 shows a representative control of a cluster of microparticles (indicated using the red square) under the influence of the controlled magnetic force and torque using (1) and (2), respectively. The input current to the electromagnetic coils is controlled by the operator using a teleoperation system [26–28]. The blue squares indicate the positions of cell mockups that are used to test the magnetic-based motion control system. At time, instant $t = 0$ seconds, the cluster starts to move toward the cell mockups. The cell mockups are subjected to the following non-contact force $\mathbf{F}_{\mathrm{nc}}(\mathbf{P}_{\mathrm{c}})$ due to the pressure gradient that is caused by the motion of the cluster:

$$\mathbf{F}_{\mathrm{nc}}(\mathbf{P}_{\mathrm{c}}) = m\left(\frac{P_{\mathrm{h}} - P_{\mathrm{l}}}{\rho_{\mathrm{f}} d}\right)\hat{\mathbf{n}}, \tag{4}$$

where P_{h} and P_{l} are the high and low pressures on the cell mockup due to the motion of the cluster and $\hat{\mathbf{n}}$ and m are a unit vector of the velocity of the cell mockup and the mass of the

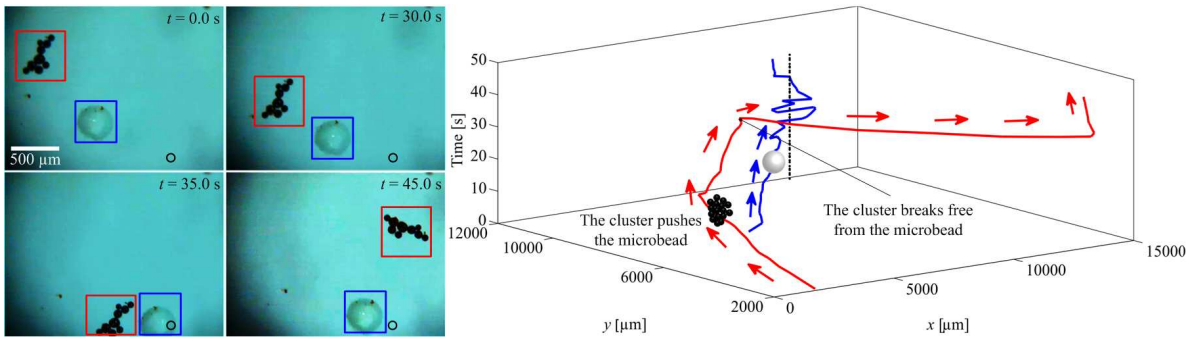

Figure 6. A representative teleoperation experiment of non-contact pushing of a cell mockup towards a reference position using a cluster of microparticles at different time instants (t). The cluster pushes the cell mockup under the influence of the controlled magnetic fields. In this micromanipulation experiment, the velocity of the cluster is 494 μm/s and 2129 μm/s before and after the positioning of the cell mockup, respectively. The average velocity of the bead is 219 μm/s. The red and blue rectangles represent the position of the cluster and the cell mockup, respectively. The cross hair indicates the reference position. The graph (right) plots the trajectory of both the cluster and the cell mockup throughout the experiment. Paramagnetic microparticles with average diameter of 100 μm are used in this experiment [29].

fluid, respectively. Further, d is the distance between the cluster and the cell mockup and $\mathbf{P}_c$ is the position of the cell mockup. The distance (d) affects the wireless manipulation.

The distance between the cluster of microparticles and the cell mockup influences the non-contact force (4). We calculate the average speed of the cell mockup versus its distance with the cluster, as shown in Fig. 5. We observe the following cases for a cluster of ten microparticles and a cell mockup with average diameter of 100 μm:

- Adhesive force is dominant (d <1200 μm): The adhesive forces attract the cell mockup to the cluster of microparticles for distance of approximately 1200 μm. In this case, the cluster can be controlled to achieve contact manipulation of the cell mockup. However, it is difficult to break free from the adhesive forces to achieve successful release at a reference position.
- Non-contact force exists (1200 μm< d <6200 μm): In this range, the cluster generates enough non-contact force to overcome the drag force on the cell mockup, and hence, non-contact pushing and pulling can be achieved.
- Zero interaction forces (d >6200 μm): At this distance, the cluster of microparticles cannot exert a non-contact force to pull or push the cell mockup.

2.2. Non-contact manipulation of cell mockups

The non-contact manipulation of the cell mockups is done using an electromagnetic system with closed configuration [22]. This system consists of four orthogonal electromagnetic coils that are controlled independently (Fig. 2). The electromagnetic coils surround a reservoir that contains the paramagnetic microparticles and the cell mockups. A microscopic system and a feature tracking algorithm are used to provide visual feedback to the control system [21]. The feature tracking algorithm determines the positions of the paramagnetic microparticle and the cell mockup, as shown in Fig. 6.

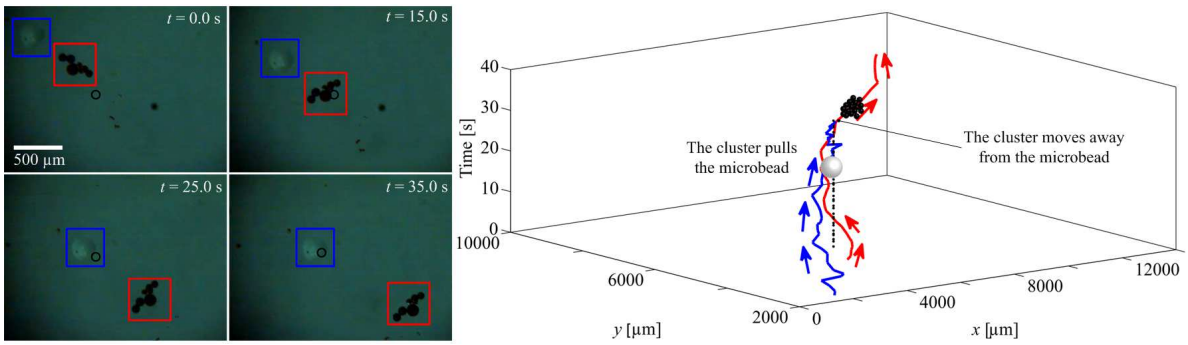

Figure 7. A representative teleoperation experiment of non-contact pulling of a cell mockup toward a reference position using a cluster of microparticles at different time instants (t). The cluster pulls the cell mockup under the influence of the controlled magnetic fields. In this micromanipulation experiment, the average velocity of the cluster is 298 μm/s and 854 μm/s before and after the positioning of the cell mockup at the reference position, respectively. The average speed of the cell mockup is 258 μm/s. The red and blue rectangles represent the position of the cluster and the cell mockup, respectively. The cross hair indicates the reference position. The graph (right) plots the trajectory of both the cluster and the cell mockup throughout the experiment. Paramagnetic microparticles with average diameter of 100 μm are used in this experiment [29].

http://dx.doi.org/10.5772/61686

Non-contact micromanipulation of cell mockups within the vicinity of the reference positions is done, as shown in the representative experiment in Fig 6. In this experiment, a cluster of nine microparticles is used to drive a cell mockup with a diameter of 300 μm. The average speed of the cluster is calculated to be 494 μm/s and 2129 μm/s before and after the positioning of the cell mockup at the reference position, respectively. The average speed of the cell mockup is calculated to be 219 μm/s. The time taken to drive the cell mockup from the initial position to the reference position (vertical black line) is 35 seconds. This experiment shows that the cluster achieves successful positioning and release of the cell mockup within the vicinity if the reference position has an error of 259 μm along x-axis and 66 μm along y-axis. We repeat the non-contact micromanipulation using pushing three times, and the average positioning time is calculated to be 30 seconds, whereas the average position errors are 190 μm along x-axis and 70 μm along y-axis. We observe that it is easier to release the cell mockup precisely at the reference position using non-contact pushing. However, this accuracy is affected when the cluster moves away from vicinity of the reference position and cell mockup (as shown in Fig. 6 at times, t=35 seconds and t=45 seconds).

Non-contact pulling of cell mockups is achieved, as shown in Fig. 7. A cluster of five microparticles are controlled under the influence of the magnetic field gradient and positioned between the reference position and the cell mockup. Motion of the cluster generates a pressure gradient in the fluid and achieves pulling of the cell mockup toward the reference position. The average speeds of the cluster and cell mockup are calculated to be 75 μm/s and 30 μm/s, respectively. The time taken to pull the cell mockup from its initial position to the reference position is 30 s. The cluster localizes the cell mockup within the vicinity of the reference position and also achieves successful release with an error of 300 μm along x-axis and 200 μm along y-axis. The non-contact micromanipulation using pulling is repeated three times, and the average positioning time is calculated to be 25 seconds. The average positioning time of micromanipulation using pulling is less than that using

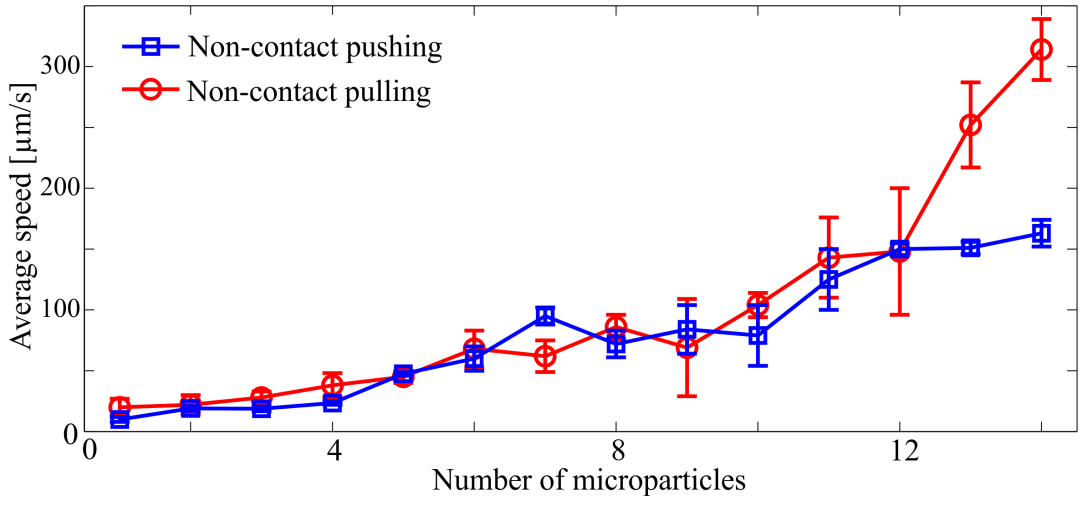

Figure 8. Average speed of the cell mockup versus the number of microparticles within the clusters. The electromagnet coil B is used to pull the cluster by the field gradients during pushing, whereas electromagnetic coil D is used during pulling. These gradients are generated by applying 1.4 A to the electromagnetic coils. The paramagnetic microparticles have an average diameter of 100 μm (PLAParticles-M-redF-plain from Micromod Partikeltechnologie GmbH, Rostock-Warnemuende, Germany) [29].

pushing since the average speed of pulling is greater than the average speed of pushing. We also observe that the non-contact micromanipulation via pulling achieves successful releases easily as in the non-contact pushing. The average position errors are calculated to be 110 μm along x-axis and 45 μm along y-axis.

The speed of the cluster of microparticles during non-contact pushing and pulling affects the release of the cell mockup and the positioning accuracy. During the micromanipulation, our control system maintains a steady speed of the cluster of microparticles. Once the cell mockup reaches the reference position, the speed of the cluster increases to break free from the non-contact forces between the cluster and the cell mockup. In the representative non-contact micromanipulation via pushing (Fig. 6), the speed of the cluster before and after the positioning of the cell mockup are 494 μm/s and 2129 μm/s, respectively. In the non-contact micromanipulation via pulling the (Fig. 7), the speeds of the cluster before and after the positioning of the cell mockup at the reference position are calculated to be 298 μm/s and 894 μm/s, respectively.

The effect of the number of microparticles within the cluster on the velocity of the cell mockup during pushing and pulling is analyzed. This analysis is done by pulling the cluster by the field gradients and measuring the linear velocity of the cell mockup for different numbers of microparticles. The number of microparticles per cluster is varied from 2 to 16 microparticles. The average speed is calculated from five pushing and pulling trials. One electromagnet is used in pushing and pulling to drive the cluster along x-axis. In these experiments, cell mockups with similar size are used, and the non-contact pulling and pushing are done between similar initial and final positions within the workspace of our magnetic system for all trails. In addition, the distance between the cluster of microparticles and the center of the cell mockup is kept constant during the calculation of the data provided in Fig. 8.

3. Manipulation and penetration of MCF-7 cells

Targeted drug delivery can be achieved by coating magnetic microparticles and nanoparticles with chemotherapeutic agents and localizing these particles within the vicinity of diseased cells. Two strategies have been proposed to release the drugs once the carriers are

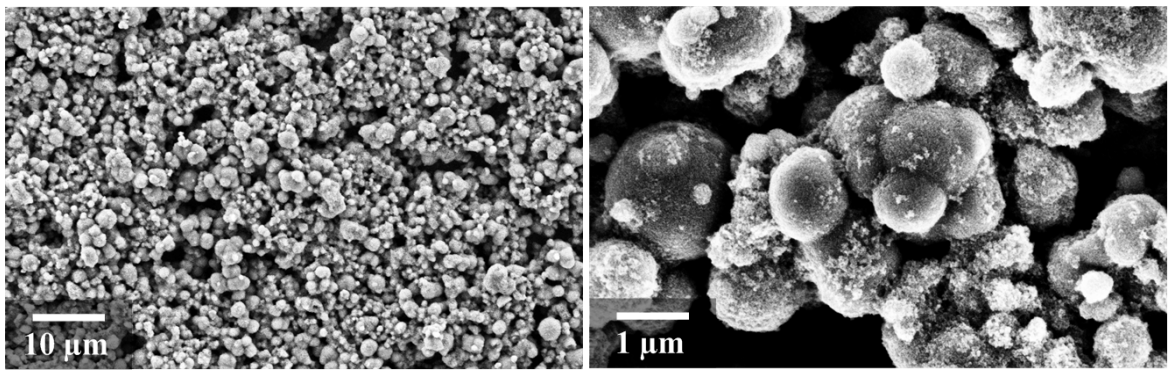

Figure 9. Scanning Electron Microscopy images of iron oxide nanoparticles. The nanoparticles ranges from 250 nm to 1 μm in diameter. These nanoparticles are pulled under the influence of the magnetic field gradient toward the MCF-7 cells.

http://dx.doi.org/10.5772/61686

concentrated at the diseased cell, namely, enzymatic activity-based approach and change of the physiological conditions approach [23]. Under certain physiological conditions, nanoparticles start releasing drug molecules in approximately 45 min and finish in 3 h [24]. Therefore, we control the motion of the nanoparticles toward MCF-7 cell to penetrate its walls or to be taken up by the cell.

3.1. Fabrication of the magnetic nanoparticles

First, a mixture of 0.675 g of iron chloride hexahydrate ($FeCl_3 \cdot H_2O$), 19 ml of ethylene glycol, 1.8 g of sodium acetate (NaAc), and 1.0 g of polyethylene glycol is stirred for 30 min. Second, the mixture is sealed in a teflon-lined stainless-steel autoclave. The autoclave is heated to a temperature of 200°C for 8 h and then cooled to room temperature. Finally, the particles are washed several times with ethanol and dried at 60°C. Fig. 9 provides scanning electron microscopy images of the fabricated iron oxide nanoparticles. These nanoparticles are controlled using (1) and (2) toward the MCF-7 cells.

3.2. Preparation of the MCF-7 cells

MCF-7 cells are cultured in RPMI 1640 media (Lonza, 12-702F) containing 10% fetal bovine serum (FBS) (Lonza, 14-802F) and 1% penicillin-streptomycin (Lonza, 17-602E). The cells

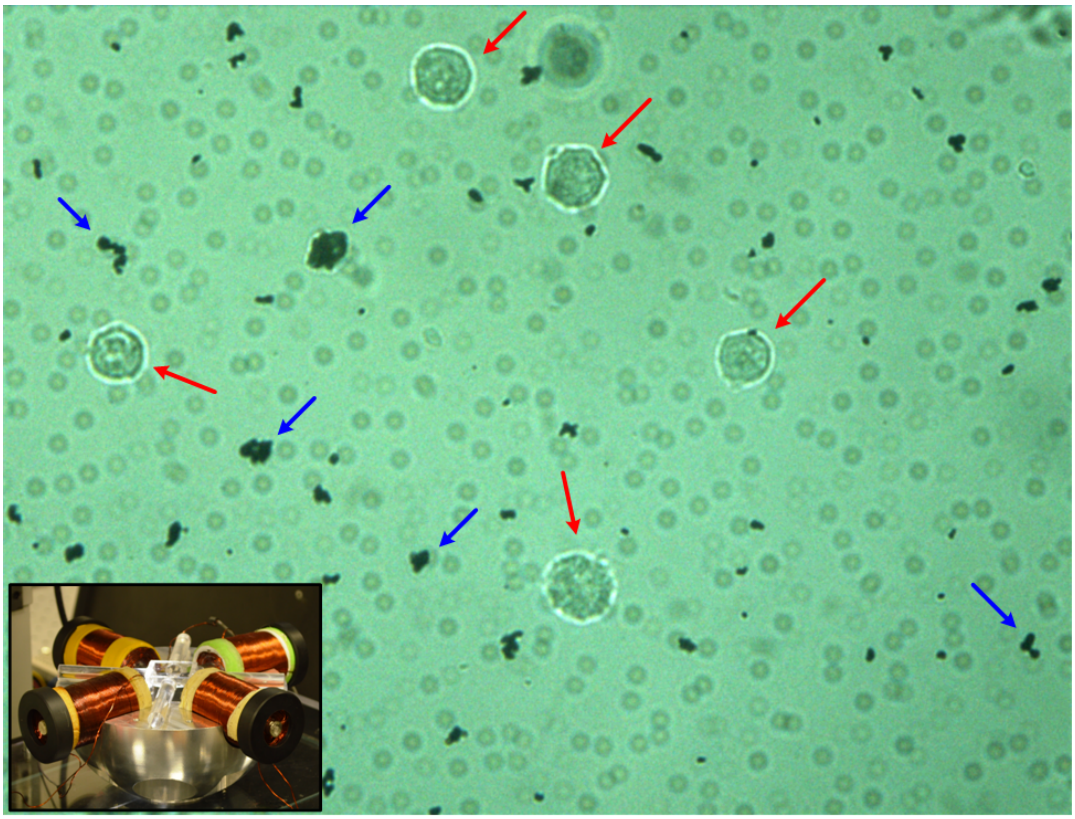

Figure 10. Microscopic image of MCF-7 cells (red arrows) and clusters of iron oxide nanoparticles (blue arrows). The nanoparticles are controlled under the influence of the magnetic field gradients. These gradients are generated using the electromagnetic system in the inset.

are incubated at 5% CO_2 and 37°C (Galaxy 170R) until they reach 80–90% confluency. Cells are washed twice using phosphate-buffered saline (PBS) (Lonza, 17-516F), followed by trypsinization (Lonza, CC-5002) and re-suspension in 10 ml RPMI. The cell suspension is then centrifuged (MIKRO, 22R) at 121xg for 5 min at 18°C. The supernatant is aspirated, and the cell pellet is re-suspended in fresh medium. Approximately 0.25×10^6 cells are mounted as cell suspension together with the nanoparticles in a ratio of 1:10 on a microscopic slide for further processing.

3.3. Cell Penetration using nanoparticles

The iron oxide nanoparticles and the MCF-7 cells are contained in a Petri dish, and the motion of the nanoparticles is controlled using the magnetic field gradient. Fig. 10 provides a microscopic image of the MCF-7 cells (red arrows) and the clusters of nanoparticles (blue arrows). Our magnetic-based control system allows us to selectively target any of the cells using a cluster of nanoparticles. The cluster is pulled toward one of MCF-7 cells using the controlled magnetic force (1), as shown in Fig. 11. At time, t=4 seconds, contact is achieved between the cluster and the cell. At this instant, our electromagnetic system exerts larger magnetic force on the dipole moment of the cluster to penetrate the wall of the cell. We observe that the cluster is taken up by the cell at time, t=22 seconds. Once the nanoparticles are ingested by the cell, they stop moving since the exerted magnetic force is not large enough to move them inside the cell.

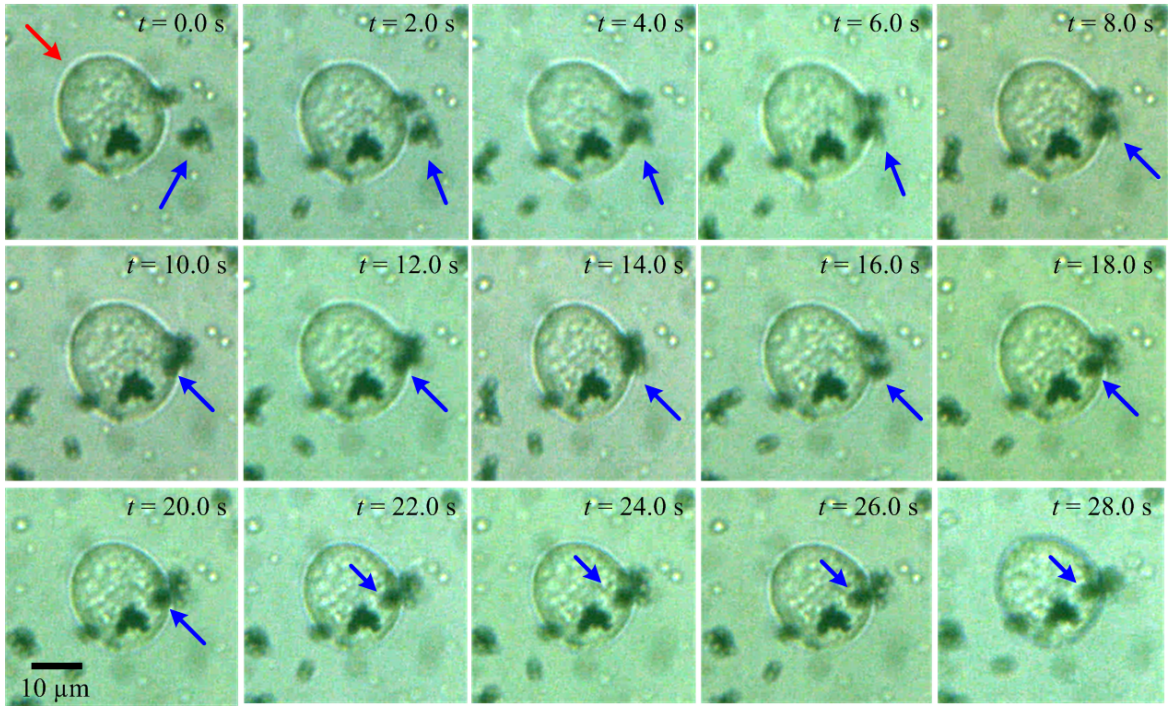

Figure 11. Penetration of MCF-7 cell (red arrow) using a cluster (blue arrow) of iron oxide nanoparticles is achieved. The cluster is pulled toward the cell under the influence of the magnetic field gradient and penetration (initial contact) of the cell is achieved at time, t=6.0 seconds. The cluster of nanoparticles is partially taken up by the cell at time, t=28 seconds.

http://dx.doi.org/10.5772/61686

The ability to move the nanoparticles toward the living MCF-7 cell and penetrate its wall holds promise for medicine. These nanoparticles can be coated with a chemotherapeutic agent and selectively controlled to target and destroy the diseased cells that engulf them. Despite the progress in fabrication of drug carriers and penetration of the MCF-7 cells, numerous challenges remain for translating this work into in vivo applications. It is necessary to achieve the motion control of the nanoparticles using feedback provided by an imaging modality, for instance, [33–35]. Fig. 12 provides a proof-of-concept result of the imaging of paramagnetic microparticles using an ultrasound system (Siemens ACUSON S2000, Siemens Healthcare, Mountain View, California, USA). We observe that the motion of the microparticles with average diameter of 100 μm and clusters of nanoparticles can be detected as artifact. Therefore, an ultrasound system can be used to achieve motion control of the nanoparticles and selective penetration of the living MCF-7 cells [32].

4. Conclusions and future work

We demonstrate experimentally the non-contact manipulation of cell mockups using paramagnetic microparticles under the influence of the controlled magnetic field gradients. At $R_e < 0.1$, the non-contact manipulation is achieved by the fluid that is carried by the controlled paramagnetic microparticle. This strategy allows us to achieve non-contact pulling and non-contact pushing of the cell mockup at average speeds of 20 μm/s and 10 μm/s, respectively. At $R_e > 0.1$, clusters of microparticles cause pressure gradient within their vicinity. This pressure is also used to move the cell mockup without contact. We observe that a cluster of 14 microparticles achieves non-contact pulling and non-contact pushing of a cell mockup at average speeds of 310 μm/s and 160 μm/s, respectively. We also demonstrate that iron oxide nanoparticles (with maximum diameter of approximately 1 μm) can penetrate a living MCF-7 cell under the influence of the magnetic field gradient exerted on the dipole moment of the nanoparticles. The nanoparticles are taken up by the MCF-7 cell in approximately 28 s.

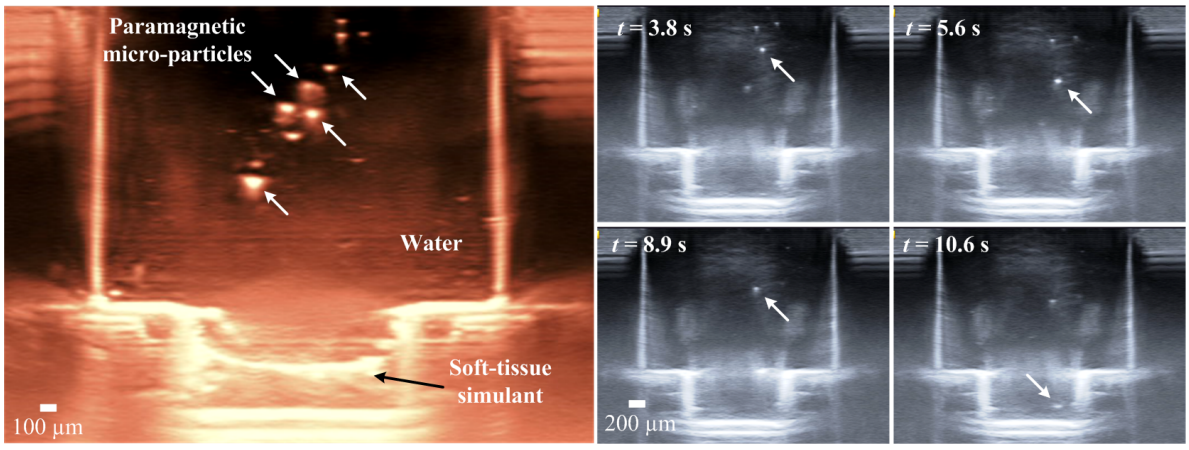

Figure 12. Ultrasound imaging of paramagnetic microparticles (PLAParticles-M-redF-plain from Micromod Partikeltechnologie GmbH, Rostock-Warnemunde, Germany). The microparticles moves under the influence of the gravitational forces inside a reservoir of water and soft-tissue simulant. This representative experiment is done using an ultrasound system (Siemens ACUSON S2000, Siemens Healthcare, Mountain View, California, USA). The insets show the motion (in real-time) of microparticles at different time instants (t).

As part of future studies, the iron oxide nanoparticles will be coated with chemotherapeutic agents and controlled toward MCF-7 and U-373 MG cells. In addition, our control system will be adapted to allow for selective targeting of certain MCF-7 and U-373 MG cells. The electromagnetic system will also be redesigned to incorporate an ultrasound imaging modality to provide feedback to the system.

5. Acknowledgements

The authors acknowledge the funding from the German University in Cairo. The research leading to these results has also received funding from the DAAD-BMBF funding project.

The authors thank Dr. Rasha M. El-Nashar and Ms. Mariam Ayoub for preparing the iron oxide nanoparticles used in Fig. 9. They would also like to thank Mr. Hazem Salah and Ms. Aya Sameh for collecting the data used in Figs. 10 and 11.

Author details

Islam S. M. Khalil[1*], Iman E. O. Gomaa[1], Reham M. Abdel-Kader[1] and Sarthak Misra[2,3]

*Address all correspondence to: islam.shoukry@guc.edu.eg

1 The German University in Cairo, Egypt

2 University of Twente, The Netherlands

3 University of Groningen and University Medical Centre Groningen, The Netherlands

References

[1] Q. A. Pankhurst, J. Connolly, S. K. Jones, and J. Dobson, "Applications of magnetic nanoparticles in biomedicine," *Journal of Physics*, vol. 36, no. 13, pp. 167–181, June 2003.

[2] M. P. Kummer, J. J. Abbott, B. E. Kartochvil, R. Borer, A. Sengul, and B. J. Nelson, "OctoMag: an electromagnetic system for 5-DOF wireless micromanipulation," *IEEE Transactions on Robotics*, vol. 26, no. 6, pp. 1006–1017, December 2010.

[3] S. Martel, O. Felfoul, J.-B. Mathieu, A. Chanu, S. Tamaz, M. Mohammadi, M. Mankiewicz, and N. Tabatabaei, "MRI-Based medical nanorobotic platform for the control of magnetic nanoparticles and flagellated bacteria for target interventions in human capillaries," *The International Journal of Robotics Research*, vol. 28, no. 9, pp. 1169–1182, September 2009.

[4] D. Popa and E. Stephanou, "Micro and meso scale robotic assembly," *Journal of Manfacturing Processes*, vol. 6, no. 1, pp. 52–71, September 2004.

[5] I. S. M. Khalil, F. van den Brink, O. S. Sukas, and S. Misra, "Microassembly using a cluster of paramagnetic microparticles," in *Proceedings of the IEEE International Conference on Robotics and Automation (ICRA)*, pp. 5507–5512, Karlsruhe, Germany, May 2013.

http://dx.doi.org/10.5772/61686

[6] S. Martel and M. Mohammadi, "Towards mass-scale micro-sssembly systems using magnetotactic bacteria," *International Manufacturing Science and Engineering Conference (ASME)*, vol. 2, no. 6, pp. 487–492, Oregon, USA, June 2011.

[7] S. Martel, C. C. Tremblay, S. Ngakeng, and G. Langlois, "Controlled manipulation and actuation of micro-objects with magnetotactic bacteria," *Applied Physics Letters*, vol. 89, no. 23, pp. 1–3, January 2007.

[8] S. Martel and M. Mohammadi, "Using a swarm of self-propelled natural microrobots in the form of flagellated bacteria to perform complex micro-assembly tasks," *in Proceedings of The IEEE International Conference on Robotics and Automation (ICRA)*, pp. 500–505, Alaska, USA, May 2010.

[9] B. K. Chen, Y. Zhang, Y. Sun, "Active release of microobjects using a MEMS microgripper to overcome adhesion forces," *Journal of Microelectromechanical Systems*, vol. 18, no. 3, pp. 652–659, May 2009.

[10] S. Saito, H. Himeno, and K. Takahashi, "Electrostatic detachment of an adhering particle from a micromanipulated probe," *Applied Physics Journal*, vol. 93, no. 4, 2219, January 2003.

[11] K. Kim, X. Liu, Y. Zhang, and Y. Sun, "Nanonewton force-controlled manipulation of biological cells using a monolithic MEMS microgripper with two-axis force feedback," *Journal of Micromechanics and Microengineering*, vol. 18, no.5, pp. 055013, May 2008.

[12] B. E. Kratochvil, M. P. Kummer, S. Erni, R. Borer, D. R. Frutiger, S. Schüurle, and B. J. Nelson, "MiniMag: a hemispherical electromagnetic system for 5-DOF wireless micromanipulation," *Proceeding of the 12th International Symposium on Experimental Robotics*, New Delhi, India, December 2010.

[13] E. Avci, H. Yabugaki, T. Hattori, K. Kamiyama, M. Kojima, Y. Mae, and T. Arai, "Dynamic releasing of biological cells at high speed using parallel mechanism to control adhesion forces," in *Proceedings of The IEEE International Conference on Robotics and Automation (ICRA)*, Hong Kong, China, May 2014.

[14] S. Floyd, C. Pawashe, and M. Sitti, "Two-dimensional contact and noncontact micromanipulation in liquid using an untethered mobile magnetic microrobot," *IEEE Transactions on Robotics*, vol. 25, no. 6, pp. 1332–1342, December 2009.

[15] I. S. M. Khalil, R. M. P. Metz, B. A. Reefman, and S. Misra, "Magnetic-Based minimum input motion control of paramagnetic microparticles in three-dimensional space," in *Proceedings of the IEEE/RSJ International Conference of Robotics and Systems (IROS)*, pp. 2053–2058, Tokyo, Japan, November 2013.

[16] I. S. M. Khalil, M. P. Pichel, L. Zondervan, L. Abelmann, and S. Misra, "Characterization and control of biological microrobots," in *Proceedings of the 13th International Symposium on Experimental Robotics-Springer Tracts in Advanced Robotics*, Quebec City, Canada, June 2012.

[17] D. Li and Y. Xia. "Electrospinning of nanofibers: reinventing the wheel?" *Advanced Materials*, vol. 16, no. 14, pp. 1151–1170, July 2004.

[18] T. H. Boyer, "The force on a magnetic dipole," *American Journal of Physics*, vol. 56, no. 8, pp. 688–692, August 1988.

[19] S. S. Shevkoplyas, A. C. Siegel, R. M. Westervelt, M. G. Prentiss, and G. M. Whitesides, "The force acting on a superparamagnetic bead due to an applied magnetic field," *Lab on a Chip*, vol. 7, no. 6, pp. 1294–1302, July 2007.

[20] H. C. Berg, "Random Walks in Biology," *Princeton University Press*, 1993.

[21] I. S. M. Khalil, V. Magdanz, S. Sanchez, O. G. Schmidt, and S. Misra, "The control of self-propelled microjets inside a microchannel with time-varying flow rates," *IEEE Transactions on Robotics*, vol. 30, no. 1, pp. 49–58, February 2013.

[22] I. S. M. Khalil, L. Abelmann, and S. Misra, "Magnetic-based motion control of paramagnetic microparticles with disturbance compensation," *IEEE Transactions on Magnetics*, vol. 50, no. 10, pp. 5400110, October 2014.

[23] C. Alexiou, W. Arnold, R. J. Klein, F. G. Parak, P. Hulin, C. Bergemann, W. Erhardt, S. Wagenpfeil, and A. S. Lübbe, "Locoregional cancer treatment with magnetic drug targeting," *Cancer Research*, vol. 60, pp. 6641–6648, December 2000.

[24] S. R. Rudge, T. L. Kurtz, C. R. Vessely, L. G. Catterall, and D. L. Williamson, "Preparation, characterization, and performance of magnetic iron-carbon composite microparticles for chemotherapy," *Biomaterials*, vol. 21, no. 14, pp. 1411–1420, July 1999.

[25] S. S. Shevkoplyas, A. C. Siegel, R. M. Westervelt, M. G. Prentiss, and G. M. Whitesides, "The force acting on a superparamagnetic bead due to an applied magnetic field," *Royal Society of Chemistry*, vol. 7, no. 6, pp. 1294–1302, July 2007.

[26] Y. Xie, D. Sun, C. Liu, H. Y. Tse and S. H. Cheng, "A force control approach to a robot-assisted cell microinjection system," in *The International Journal of Robotics Research*, vol. 29, no. 9, pp. 322–331, November 2009.

[27] K. Takeo and K. Kosuge, "Implementation of the micro-macro teleoperation system without using slave-side force sensors," in *Proceedings of the IEEE International Conference on Robotics and Automation (ICRA)*, pp. 1600–1605, Albuquerque, USA, April 1997.

[28] A. Bolopion, H. Xie, D. S. Haliyo, and Stéphane Régnier, "Haptic teleoperation for 3-D microassembly of spherical objects," in *IEEE/ASME Transactions on Mechatronics*, vol. 17, no. 1, pp. 116–127, December 2010.

[29] A. G. El-Gazzar, L. E. Al-Khouly, A. Klingner, S. Misra and I. S. M. Khalil, "Non-Contact manipulation of microbeads via pushing and pulling using magnetically controlled clusters of paramagnetic microparticles," in *Proceedings of the IEEE/RSJ International Conference of Robotics and Systems (IROS)*, pp. 778–783, Hamburg, Germany, September 2015.

http://dx.doi.org/10.5772/61686

[30] A. Hosney, A. Klingner, S. Misra, and I. S. M. Khalil, "Propulsion and steering of helical magnetic microrobots using two synchronized rotating dipole fields in three-dimensional space," in *Proceedings of the IEEE/RSJ International Conference of Robotics and Systems (IROS)*, pp. 1988–1993, Hamburg, Germany, September 2015.

[31] I. S. M. Khalil, V. Magdanz, S. Sanchez, O. G. Schmidt and S. Misra, "Magnetotactic bacteria and microjets: a comparative study," in *Proceedings of the IEEE/RSJ International Conference of Robotics and Systems (IROS)*, pp. 2035–2040, Tokyo, Japan, November 2013.

[32] I. S. M. Khalil, P. Ferreira, R. Eleutério, C. L. de Korte, and S. Misra, "Magnetic-based closed-loop control of paramagnetic microparticles using ultrasound feedback," in *Proceedings of the IEEE International Conference on Robotics and Automation (ICRA)*, pp. 3807–3812, Hong Kong, June 2014.

[33] S. Martel, O. Felfoul, J.-B. Mathieu, A. Chanu, S. Tamaz, M. Mohammadi, M. Mankiewicz, and N. Tabatabaei , "MRI-based medical nanorobotic platform for the control of magnetic nanoparticles and flagellated bacteria for target interventions in human capillaries," *International Journal of Robotics Research*, vol. 28, no. 9, pp. 1169–1182, September 2009.

[34] J.-B. Mathieu and S. Martel, "Steering of aggregating magnetic microparticles using propulsion gradients coils in an MRI scanner," *Magnetic Resonance in Medicine*, vol. 63, no. 5, pp. 1336–1345, May 2010.

[35] M. Evertsson, M. Cinthio, S. Fredriksson, F. Olsson, H. W. Persson, and T. Jansson, "Frequency- and phase-sensitive magnetomotive ultrasound imaging of superparamagnetic iron oxide nanoparticles," in *IEEE Transactions on Ultrasonics, Ferroelectrics, and Frequency Control*, vol. 60, no. 3, pp. 481–491, March 2013.